Molecular Cell, Volume *82*

Supplemental information

Distal and proximal *cis*-regulatory elements sense X chromosome dosage and developmental state at the *Xist* locus

Rutger A.F. Gjaltema, Till Schwämmle, Pauline Kautz, Michael Robson, Robert Schöpflin, Liat Ravid Lustig, Lennart Brandenburg, Ilona Dunkel, Carolina Vechiatto, Evgenia Ntini, Verena Mutzel, Vera Schmiedel, Annalisa Marsico, Stefan Mundlos, and Edda G. Schulz

Figure S1

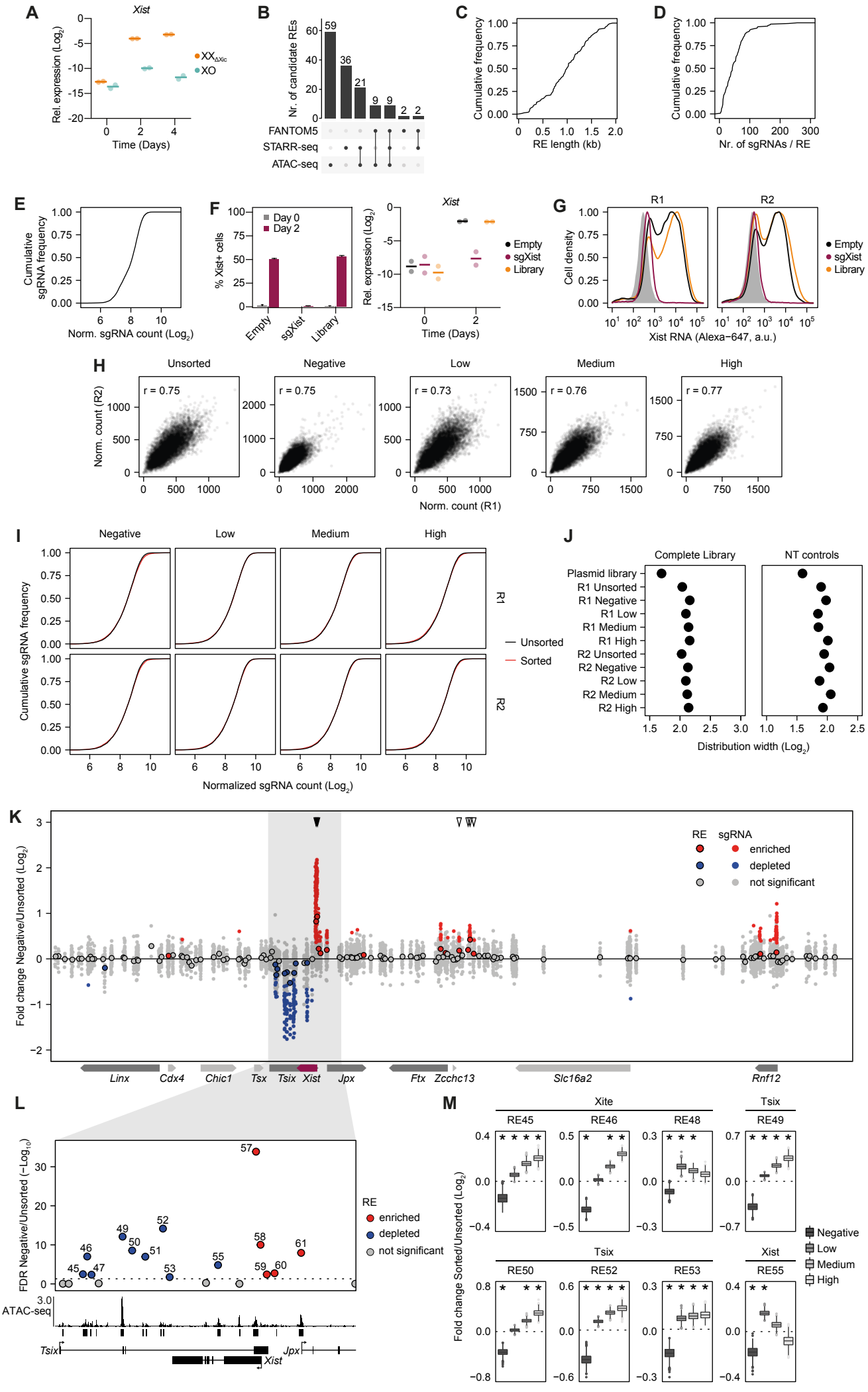
A
Xist
Rel. expression (Log2)
Time (Days)
XXΔXic
XO
B
Nr. of candidate REs
59
36
21
9
9
2
2
FANTOM5
STARR-seq
ATAC-seq
C
Cumulative frequency
RE length (kb)
D
Cumulative frequency
Nr. of sgRNAs / RE
E
Cumulative sgRNA frequency
Norm. sgRNA count (Log2)
F
Day 0
Day 2
% Xist+ cells
Empty
sgXist
Library
Xist
Rel. expression (Log2)
Time (Days)
G
R1
R2
Cell density
Xist RNA (Alexa−647, a.u.)
H
Unsorted
Negative
Low
Medium
High
r = 0.75
r = 0.75
r = 0.73
r = 0.76
r = 0.77
Norm. count (R2)
Norm. count (R1)
I
Cumulative sgRNA frequency
Unsorted
Sorted
Normalized sgRNA count (Log2)
J
Complete Library
NT controls
Plasmid library
R1 Unsorted
R1 Negative
R1 Low
R1 Medium
R1 High
R2 Unsorted
R2 Negative
R2 Low
R2 Medium
R2 High
Distribution width (Log2)
K
Fold change Negative/Unsorted (Log2)
RE
sgRNA
enriched
depleted
not significant
Linx
Cdx4
Chic1
Tsx
Tsix
Xist
Jpx
Ftx
Zcchc13
Slc16a2
Rnf12
L
FDR Negative/Unsorted (−Log10)
RE
enriched
depleted
not significant
ATAC-seq
Tsix
Jpx
Xist
M
Xite
Tsix
RE45
RE46
RE48
RE49
Tsix
Xist
RE50
RE52
RE53
RE55
Fold change Sorted/Unsorted (Log2)
Negative
Low
Medium
High

Figure S1. Identification of *Xist*-regulating genomic elements through a pooled CRISPR screen (Related to Figure 1).

(A) *Xist* expression assessed by qRT-PCR as quality control, when generating ATAC-seq data showing XX-specific upregulation of *Xist* during differentiation. Dots indicate individual biological replicates (n=2) and horizontal bars the mean. (**B**) UpsetR plot showing the number of candidate REs identified from the different data sources. (**C-D**) Cumulative frequency plots showing the distribution of length (C) and the number of sgRNAs (D) across all candidate REs. (**E**) Cumulative frequency plot showing the distribution of sgRNA counts in the cloned sgRNA library. (**F-G**) Quality controls for the CRISPR screen in Fig. 1 confirming *Xist* upregulation upon transduction with the sgRNA library (Library) or the empty vector (Empty) and *Xist* repression by a control sgRNA targeting the *Xist* promoter (sgXist). *Xist* was quantified in two biological replicates by RNA-FISH (F, left), qRT-PCR (F, right) and by Flow-FISH (G). For RNA-FISH, 100 cells were counted per replicate and mean and SD are shown. For Flow-FISH both replicates (R1, R2) are shown and undifferentiated cells transduced with the sgRNA library are shaded in grey. (**H**) Scatterplots showing the correlation between the replicates in the screen for each fraction as indicated. Pearson correlation coefficients are depicted in the panels. (**I**) Cumulative frequency plots showing the distribution of the sgRNA library in the sorted fractions compared to the unsorted population. (**J**) Log_2 distribution width (fold change between the 10^{th} and 90^{th} percentiles) for all sgRNAs (left) and non-targeting (NT) sgRNAs only (right). The NT distribution width was similar across samples, suggesting that sufficient library coverage was maintained during all steps of the screen. (**K-L**) Comparison of sgRNA abundance in the Xist-negative fraction compared to the unsorted population. Small dots in (K) show individual sgRNAs and rimmed circles in (K-L) denote results from a joint analysis of all sgRNAs targeting one RE. Significantly enriched and depleted sgRNAs (*MAGeCK test,* two sided p-value <0.05) and REs (*MAGeCK mle,* Wald.FDR <0.05) are colored red and blue, respectively. Arrowheads in (K) indicate the promoter-proximal elements RE57-58 (filled) and the distal enhancers RE93, 95-97 (open). The entire region targeted in the screen is shown in (K) and a zoom-in around *Xist* in (L). In (L) ATAC-seq data is shown from differentiated $XX_{\Delta Xic}$ cells at day 2. (**M**) Log_2 fold-change of sorted and unsorted populations for 1000 bootstrap samples of 50 randomly selected sgRNAs. REs in TAD-D with an empirical FDR <0.01 (asterisks) in at least two populations are shown.

Figure S2

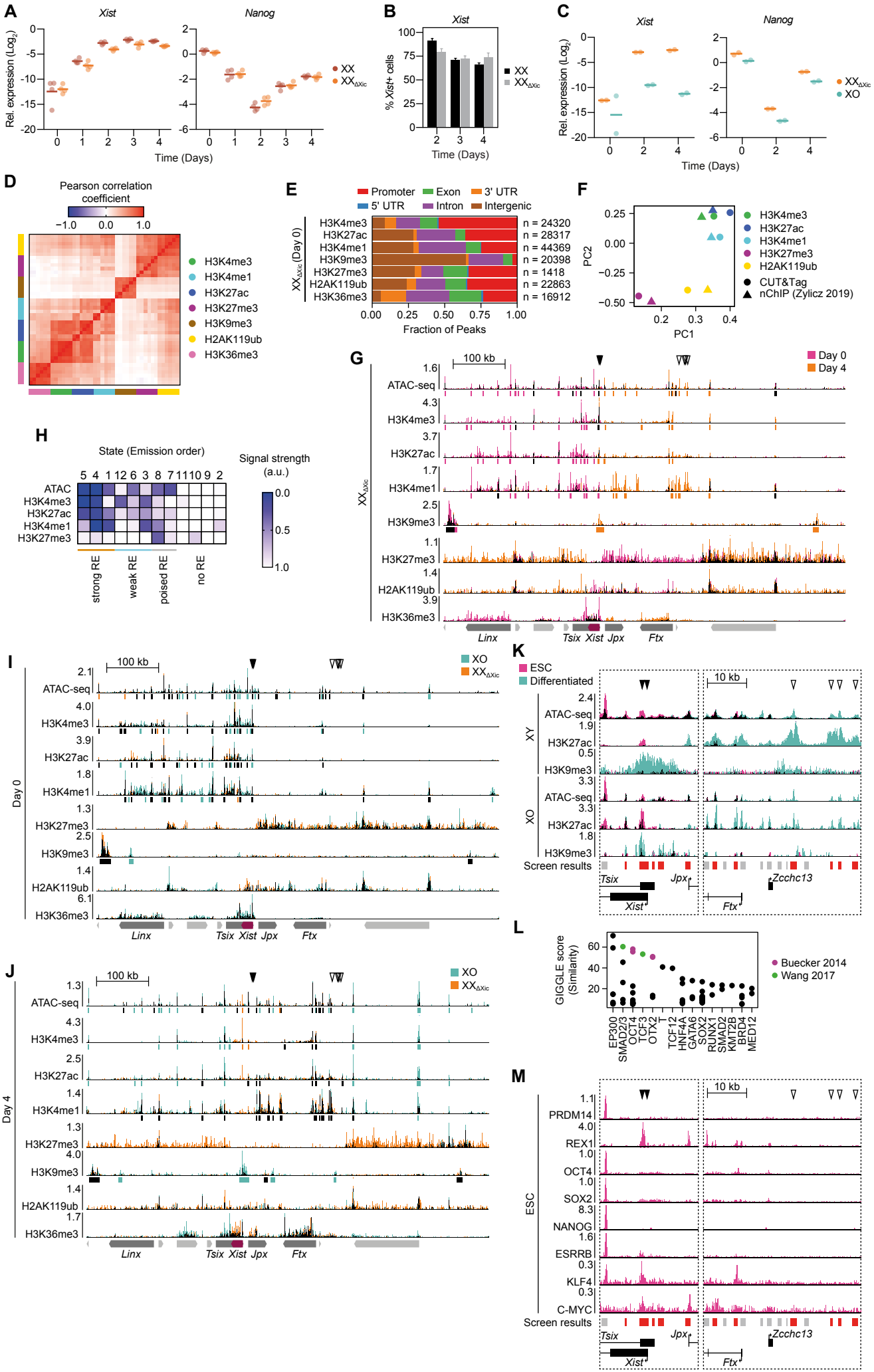
A
Xist
Nanog
Rel. expression (Log2)
Time (Days)
XX
XXΔXic
B
Xist
% Xist+ cells
Time (Days)
C
Xist
Nanog
Rel. expression (Log2)
XXΔXic
XO
Time (Days)
D
Pearson correlation coefficient
−1.0 0.0 1.0
H3K4me3
H3K4me1
H3K27ac
H3K27me3
H3K9me3
H2AK119ub
H3K36me3
E
Promoter
Exon
3' UTR
5' UTR
Intron
Intergenic
XXΔXic (Day 0)
n = 24320
n = 28317
n = 44369
n = 20398
n = 1418
n = 22863
n = 16912
Fraction of Peaks
F
PC2
PC1
H3K4me3
H3K27ac
H3K4me1
H3K27me3
H2AK119ub
CUT&Tag
nChIP (Zylicz 2019)
G
100 kb
Day 0
Day 4
XXΔXic
ATAC-seq
H3K4me3
H3K27ac
H3K4me1
H3K9me3
H3K27me3
H2AK119ub
H3K36me3
Linx
Tsix Xist Jpx
Ftx
H
State (Emission order)
5 4 1 12 6 3 8 7 11 10 9 2
ATAC
H3K4me3
H3K27ac
H3K4me1
H3K27me3
strong RE
weak RE
poised RE
no RE
Signal strength (a.u.)
0.0
0.5
1.0
I
100 kb
XO
XXΔXic
Day 0
ATAC-seq
H3K4me3
H3K27ac
H3K4me1
H3K27me3
H3K9me3
H2AK119ub
H3K36me3
Linx
Tsix Xist Jpx
Ftx
J
100 kb
XO
XXΔXic
Day 4
ATAC-seq
H3K4me3
H3K27ac
H3K4me1
H3K27me3
H3K9me3
H2AK119ub
H3K36me3
Linx
Tsix Xist Jpx
Ftx
K
ESC
Differentiated
10 kb
XY
XO
ATAC-seq
H3K27ac
H3K9me3
Screen results
Tsix
Xist
Jpx
Ftx
Zcchc13
L
GIGGLE score (Similarity)
Buecker 2014
Wang 2017
EP300
SMAD2/3
OCT4
TCF3
OTX2
TCF12
HNF4A
GATA6
SOX2
RUNX1
SMAD2
KMT2B
BRD4
MED12
M
10 kb
ESC
PRDM14
REX1
OCT4
SOX2
NANOG
ESRRB
KLF4
C-MYC
Screen results
Tsix
Xist
Jpx
Ftx
Zcchc13

Figure S2. Differentiation cues and X-dosage control distal, and proximal REs, respectively (Related to Figure 2).

(**A-B**) qRT-PCR and RNA-FISH comparing the $XX_{\Delta Xic}$ line with the parental TX1072 cell line. In (A) dots represent 4 independent biological replicates, horizontal bars the mean. In (B) mean and SD of 3 biological replicates are shown. (**C**) qRT-PCR showing expression of *Xist* and *Nanog*, during the differentiation experiment where chromatin was profiled by CUT&Tag. Dots represent 2 independent biological replicates, horizontal bars the mean. (**D**) Heatmap showing the Pearson correlation coefficients between all CUT&Tag samples. Replicates were merged and samples ordered via hierarchical clustering. The expected correlation pattern was observed among modifications associated with active genes (H4K4me1/3, H3K27ac, H3K36me3) and among those associated with polycomb-repression (H3K27me3, H2AK119ub). (**E**) Distribution of CUT&Tag peaks in undifferentiated $XX_{\Delta Xic}$ mESCs across genomic regions as indicated. Peaks were identified with MACS2 (FDR<0.05). As expected, H3K4me3 is primarily found at promoters, H3K9me3 at intergenic regions (likely repeats) and H3K36me3 at gene bodies. The total number of peaks for each mark is indicated on the right. (**F**) PCA analysis of CUT&Tag read distribution in undifferentiated $XX_{\Delta Xic}$ cells (circles) together with native ChIP-seq data (Żylicz et al., 2019) (triangles), previously generated in the parental TX1072 cell line in the same culture conditions (2iL). **(G)** DNA accessibility and histone modifications in female $XX_{\Delta Xic}$ mESCs prior to (Day 0) and at day 4 of differentiation profiled by ATAC-seq and CUT&Tag. The tracks are overlaid in a way that an increased signal at day 0 and day 4 is colored in pink and orange as indicated, while the remaining signal is colored in black. (**H**) Heatmap showing enrichment of CUT&Tag and ATAC-seq signals in chromatin states identified using *ChromHMM*. States were ordered according to the assigned identity shown on the bottom. **(I-J)** DNA accessibility and histone modifications in $XX_{\Delta Xic}$ and XO mESCs prior to (I) and after 4 days (J) of differentiation profiled by ATAC-seq and CUT&Tag. Overall loss of activity and increased H3K27me3 specifically in $XX_{\Delta Xic}$ mESCs reflects initiation of gene silencing at the onset of XCI. **(K)** DNA accessibility, H3K27ac and H3K9me3 in XY and XO cells prior to (day 0) and during differentiation (day 2) at the *Xist* promoter area and the most prominent distal enhancer elements. XY data are profiled by ChIP-seq and differentiated towards EpiLC-fate (Bleckwehl et al., 2021). **(L)** Enrichment of ChIP-seq signals in RE93, 95-97 computed through the *Cistrome DB Toolkit*. The colored datasets are shown in Fig. 2I-J. **(M)** ChIP-seq data of pluripotency factors at the *Xist* promoter area and the most prominent distal enhancer elements. The data was collected in XX (REX1) or XY ESCs (all other factors) (Chronis et al., 2017; Gontan et al., 2012; Tu et al., 2016).

In (G,I,J) vertical bars below the tracks mark peaks identified in at least one time point and are colored corresponding to the increased condition if the signal is significantly different (FDR<0.05) between the conditions across both biological replicates. Arrowheads in (G, I-K, M) indicate the promoter-proximal elements RE57-58 (filled) and the distal enhancers RE93, 95-97 (open). The screen results (Fig. 1) are shown below the tracks in (K, M).

Figure S3

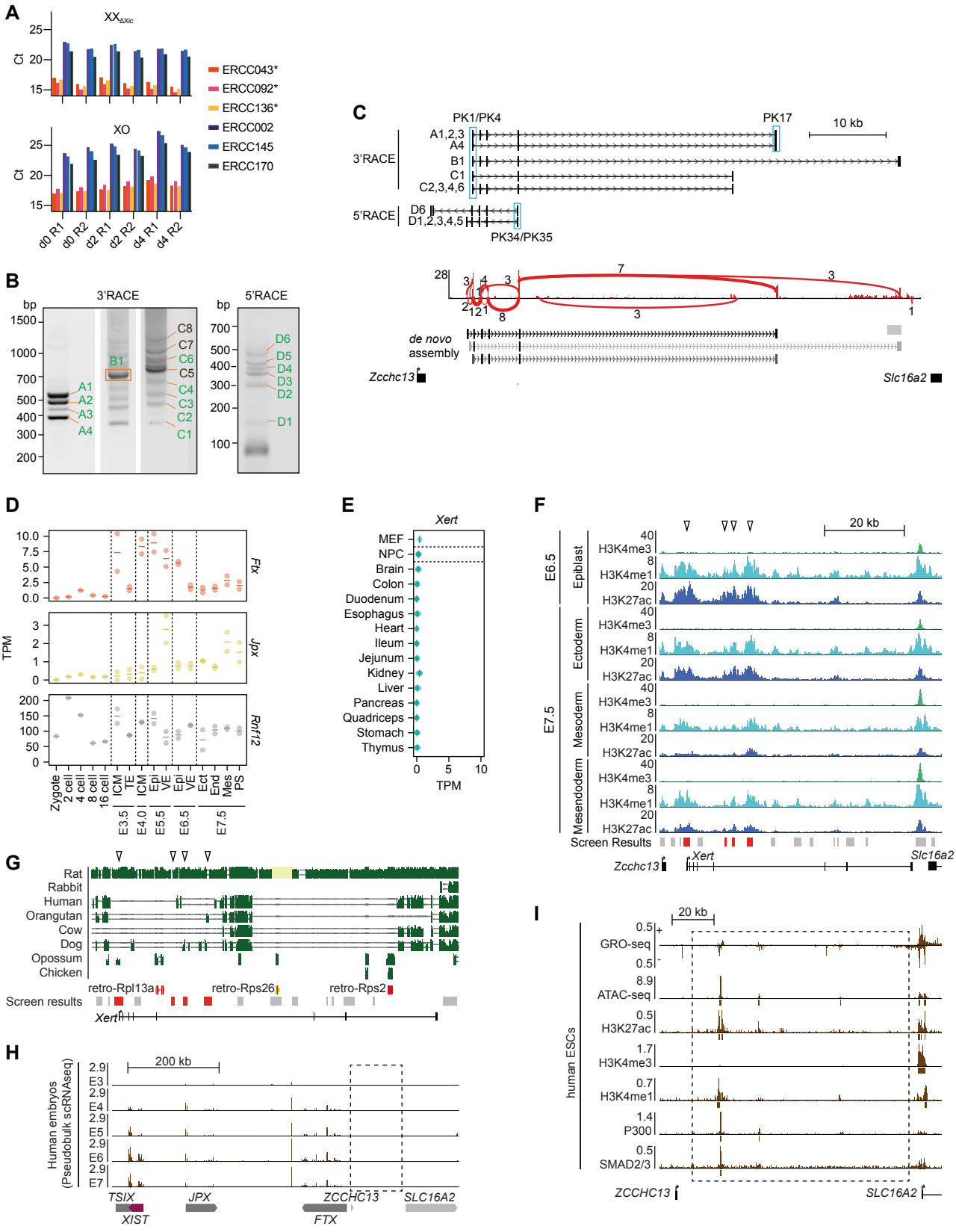
A
XXΔXic
XO
Ct
ERCC043*
ERCC092*
ERCC136*
ERCC002
ERCC145
ERCC170
d0 R1
d0 R2
d2 R1
d2 R2
d4 R1
d4 R2
B
3'RACE
5'RACE
bp
A1
A2
A3
A4
B1
C1
C2
C3
C4
C5
C6
C7
C8
D1
D2
D3
D4
D5
D6
C
PK1/PK4
PK17
10 kb
3'RACE
A1,2,3
A4
B1
C1
C2,3,4,6
5'RACE
D6
D1,2,3,4,5
PK34/PK35
de novo
assembly
Zcchc13
Slc16a2
D
Ftx
Jpx
Rnf12
TPM
Zygote
2 cell
4 cell
8 cell
16 cell
ICM
TE
ICM
Epi
VE
Epi
VE
Ect
End
Mes
PS
E3.5
E4.0
E5.5
E6.5
E7.5
E
Xert
MEF
NPC
Brain
Colon
Duodenum
Esophagus
Heart
Ileum
Jejunum
Kidney
Liver
Pancreas
Quadriceps
Stomach
Thymus
TPM
F
20 kb
E6.5
E7.5
Epiblast
Ectoderm
Mesoderm
Mesendoderm
H3K4me3
H3K4me1
H3K27ac
Screen Results
Zcchc13
Xert
Slc16a2
G
Rat
Rabbit
Human
Orangutan
Cow
Dog
Opossum
Chicken
retro-Rpl13a
retro-Rps26
retro-Rps2
Screen results
Xert
H
Human embryos
(Pseudobulk scRNAseq)
200 kb
E3
E4
E5
E6
E7
TSIX
XIST
JPX
ZCCHC13
FTX
SLC16A2
I
20 kb
human ESCs
GRO-seq
ATAC-seq
H3K27ac
H3K4me3
H3K4me1
P300
SMAD2/3
ZCCHC13
SLC16A2

Figure S3. An unannotated enhancer-associated transcript is upregulated concomitantly with *Xist* at the onset of XCI (Related to Figure 3).

(**A**) Quality controls for TT-seq data showing enrichment of S4U-labelled spike-in RNAs (asterisks) compared to unlabelled controls after biotin-pulldown, assessed by qRT-PCR. (**B-C**) Isoform detection of *Xert*. (B) Agarose gel image of 3'- and 5'-RACE. Bands that were purified and Sanger-sequenced are labelled. Bands labelled in green gave successful Sanger sequencing results, which are summarized in (C, top). Sashimi plot and *de novo* transcript assembly (C, bottom) from polyA-RNA-seq data derived from differentiated (day 2) TX1072 cells. Numerical labels of the red lines indicate the number of split reads supporting the indicated splice junction. (**D**) *Jpx, Ftx and Rnf12* RNA expression during early mouse embryonic development (Zygote-E7.5) from sex-mixed embryos (Deng et al., 2014; Zhang et al., 2018). Inner cell mass (ICM), trophectoderm (TE), epiblast (Epi), visceral endoderm (VE), ectoderm (Ect), endoderm (End), mesoderm (Mes), primitive streak (PS). **(E)** *Xert* RNA expression in sex-mixed adult mouse tissues (Söllner et al., 2017), female mouse embryonic fibroblasts (MEF) (Wang et al., 2019) and female neural progenitor cells (NPC) (Bauer et al., 2021). (**F**) ChIP-seq coverage tracks for H3K4me3, H3K4me1 and H3K27ac from E6.5 and E7.5 combined sex-mixed mouse embryos at the *Xert* locus (Yang et al., 2019). **(G)** UCSC browser tracks showing sequence conservation in selected vertebrate species around the *Xert* locus (green). **(H)** Browser tracks showing pseudobulk scRNA-seq data in sex-mixed human embryos between the *TSIX* and *SLC16A2* genes (Petropoulos et al., 2016). **(I)** Browser tracks showing nascent transcription (GRO-seq) (Wang et al., 2015), DNA accessibility (Guo et al., 2017), SMAD2/3-binding (Li et al., 2019), H3K27ac, H3K4me1, H3K4me3 and P300 binding (Rada-Iglesias et al., 2011) in human embryonic stem cells (XY or XX).

Bars in (E-F) and lines in (D) denote the mean of 2 (E-F) or 3 (D) biological replicates, dots represent individual measurements. Open arrowheads in (G) indicate the distal enhancers RE93, 95-97. The screen results (Fig. 1) are shown below the tracks in (G), where candidate REs that inhibit (blue) or activate (red) *Xist* expression in the negative or high fractions of the CRISPR screen are colored. Dashed boxes in (I-J) demarcate the approximate genomic region where *Xert* would be located in the human genome.

Figure S4

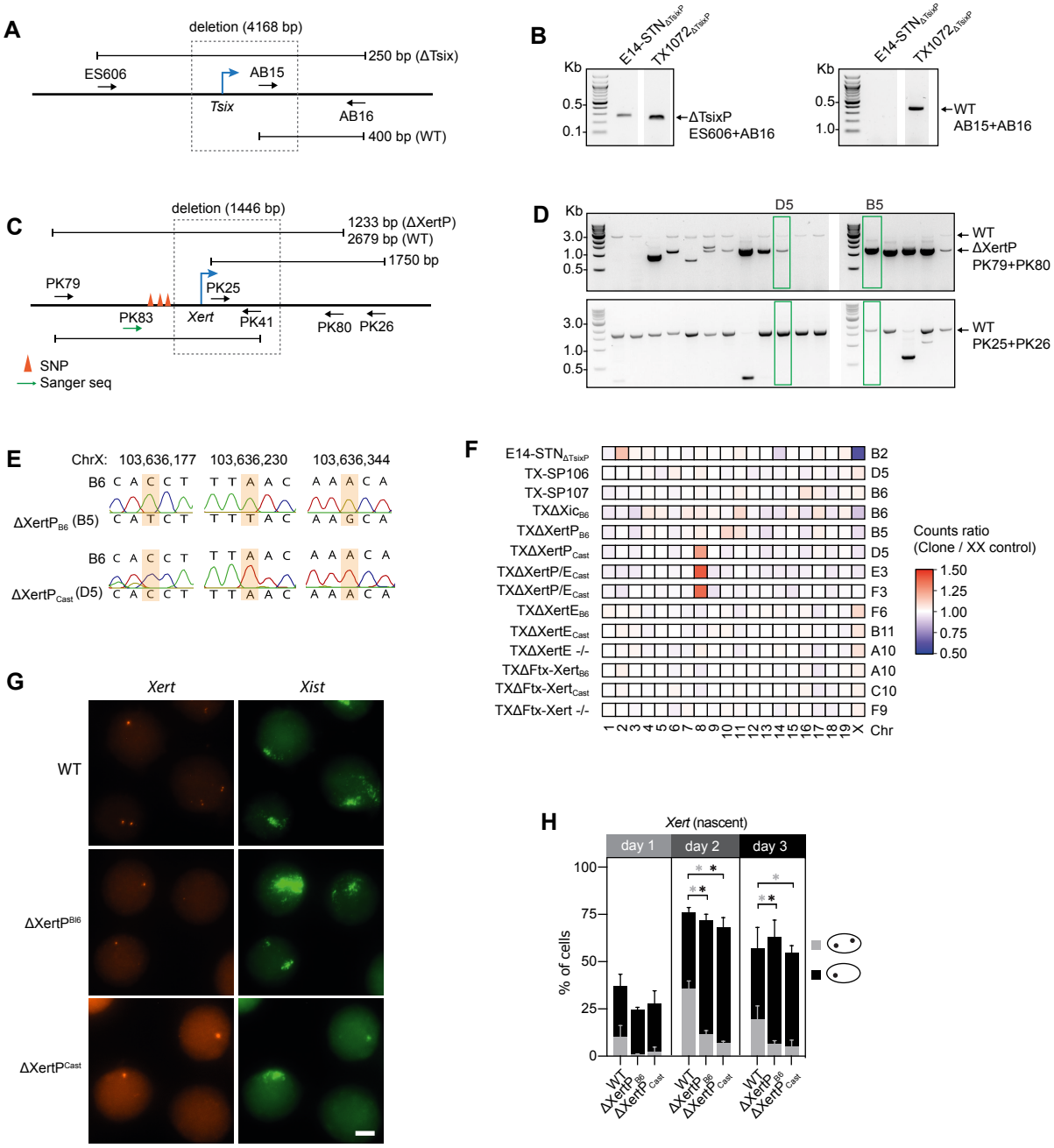
A
deletion (4168 bp)
250 bp (ΔTsix)
ES606
AB15
Tsix
AB16
400 bp (WT)
B
E14-STNΔTsixP
TX1072ΔTsixP
Kb
0.5
0.1
ΔTsixP
ES606+AB16
Kb
0.5
1.0
WT
AB15+AB16
C
deletion (1446 bp)
1233 bp (ΔXertP)
2679 bp (WT)
1750 bp
PK79
PK25
PK83
Xert
PK41
PK80
PK26
SNP
Sanger seq
D
Kb
D5
B5
3.0
1.0
0.5
WT
ΔXertP
PK79+PK80
3.0
1.0
0.5
WT
PK25+PK26
E
ChrX: 103,636,177 103,636,230 103,636,344
B6 C A C C T T T A A C A A A C A
ΔXertPB6 (B5) C A T C T T T T A C A A G C A
B6 C A C C T T T A A C A A A C A
ΔXertPCast (D5) C A C C T T T A A C A A A C A
F
E14-STNΔTsixP B2
TX-SP106 D5
TX-SP107 B6
TXΔXicB6 B6
TXΔXertPB6 B5
TXΔXertPCast D5
TXΔXertP/ECast E3
TXΔXertP/ECast F3
TXΔXertEB6 F6
TXΔXertECast B11
TXΔXertE -/- A10
TXΔFtx-XertB6 A10
TXΔFtx-XertCast C10
TXΔFtx-Xert -/- F9
1 2 3 4 5 6 7 8 9 10 11 12 13 14 15 16 17 18 19 X Chr
Counts ratio
(Clone / XX control)
1.50
1.25
1.00
0.75
0.50
G
Xert
Xist
WT
ΔXertPBl6
ΔXertPCast
H
Xert (nascent)
day 1
day 2
day 3
100
75
50
25
0
% of cells
WT
ΔXertPB6
ΔXertPCast

Figure S4. *Xert* transcription enhances *Xist* expression in *cis* (Related to Figure 4).

(**A-B**) Genotyping for E14-STN$_{\Delta TsixP}$ clones. (A) Arrows indicate primer positions. Lines denote PCR amplicons. (B) Agarose gel images of two genotyping PCRs (from E14-STN$_{\Delta TsixP}$ clones), that show the deleted (left panel) or the wt band only (right panel). (**C-E**) Genotyping of TXΔXertP clones. (C) Arrows indicate primer positions. Orange pyramids indicate the SNPs used in Sanger sequencing validation of the deleted allele. Lines indicate PCR amplicons. (D) Agarose gel images of two genotyping PCRs, that show the deletion and wt band (top) or the wt band only (bottom). Green boxes mark the clones that were selected for all further analyses. (E) Assessment of three SNPs (orange boxes) by Sanger sequencing of amplicon PK79/PK41 and PK83 as sequencing primer (see C). Chromatogram and the genomic coordinates (mm10) of the SNPs are shown for both heterozygous ΔXertP lines. (**F**) Heatmap of NGS karyotyping data for all cell lines used in the study. Counts mapping to each chromosome were normalized to an XX control cell line. (**G**) Example images of *Xert* and *Xist* RNA expression detected by RNA-FISH in two heterozygous ΔXertP lines and parental TX1072 control line (WT) differentiated for 2 days as quantified in main Fig. 4F-G. Scale bar marks 5 µm. **(H)** Quantification of *Xert* RNA using RNA-FISH following a differentiation time course of two heterozygous XertP deletion lines and the parental wildtype line (WT). 100 cells were quantified per replicate. In (H) mean and SD of 3 biological replicates are shown. Asterisks indicate significance of $p<0.05$ using an unpaired two-tailed T-test.

Figure S5

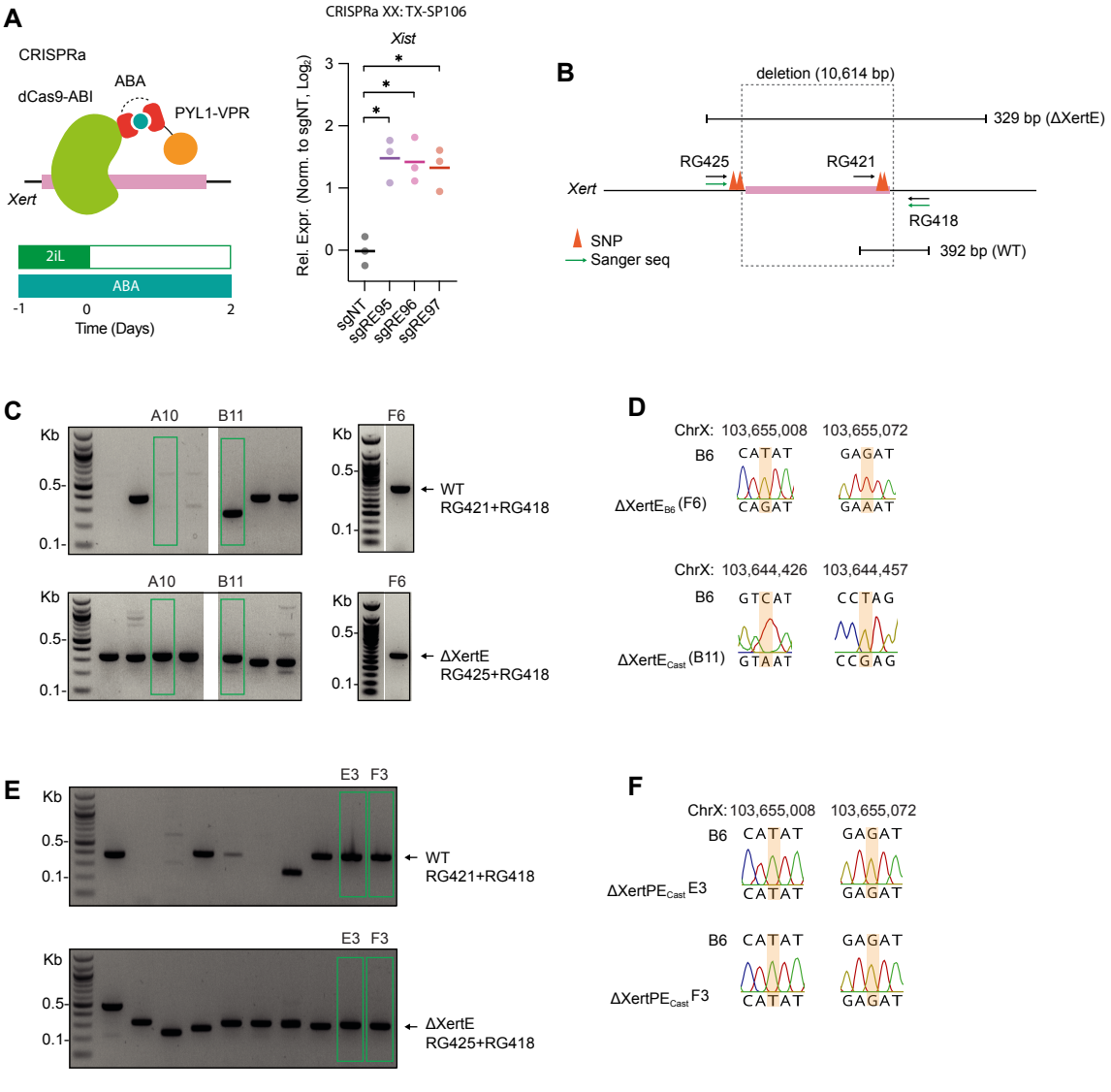
A
CRISPRa
ABA
dCas9-ABI
PYL1-VPR
Xert
2iL
ABA
-1
0
2
Time (Days)
CRISPRa XX:TX-SP106
Xist
Rel. Expr. (Norm. to sgNT, Log2)
sgNT
sgRE95
sgRE96
sgRE97
B
deletion (10,614 bp)
329 bp (ΔXertE)
RG425
RG421
Xert
RG418
SNP
Sanger seq
392 bp (WT)
C
A10
B11
F6
Kb
0.5
0.1
WT
RG421+RG418
ΔXertE
RG425+RG418
D
ChrX: 103,655,008 103,655,072
B6
CATAT
GAGAT
ΔXertE B6 (F6)
CAGAT
GAAAT
ChrX: 103,644,426 103,644,457
GTCAT
CCTAG
ΔXertE Cast (B11)
GTAAT
CCGAG
E
E3 F3
F
ChrX: 103,655,008 103,655,072
ΔXertPE Cast E3
ΔXertPE Cast F3

Figure S5. An intronic enhancer cluster within *Xert* activates *Xist* expression in *cis* (Related to Figure 5).

(**A**) Ectopic XertE activation in TX-SP106 cells stably expressing an inducible CRISPRa system and three sgRNAs from a multiguide expression vector that target one RE or non-targeting controls (NT). Relative *Xist* RNA expression after two days of differentiation was assessed by qRT-PCR (n=3) and normalized to sgNT. Horizontal bars denote the mean of 3 biological replicates; dots represent individual measurements. (**B-F**) Genotyping of the XertE deletion in ΔXertE lines (C-D) and ΔXertP/E lines (E-F), carrying a heterozygous or homozygous deletion of the *Xert* enhancer cluster. (B) Arrows indicate primer positions. The orange pyramid indicates the SNP used to identify the wt allele by Sanger sequencing in (D,F). Lines indicate PCR amplicons. (C,E) Agarose gel images of two genotyping PCRs of the ΔXertE clones with green boxes marking the clones that were selected for all further analyses. (D,F) Sanger sequencing of amplicon RG421/RG418 and RG418 as sequencing primer to identify the deleted allele in ΔXertE mESCs, except for clone B11, where amplicon RG425/RG418 was sequenced with RG425. Chromatograms of the assessed SNP (orange box) are shown with its genomic coordinate (mm10).

Figure S6

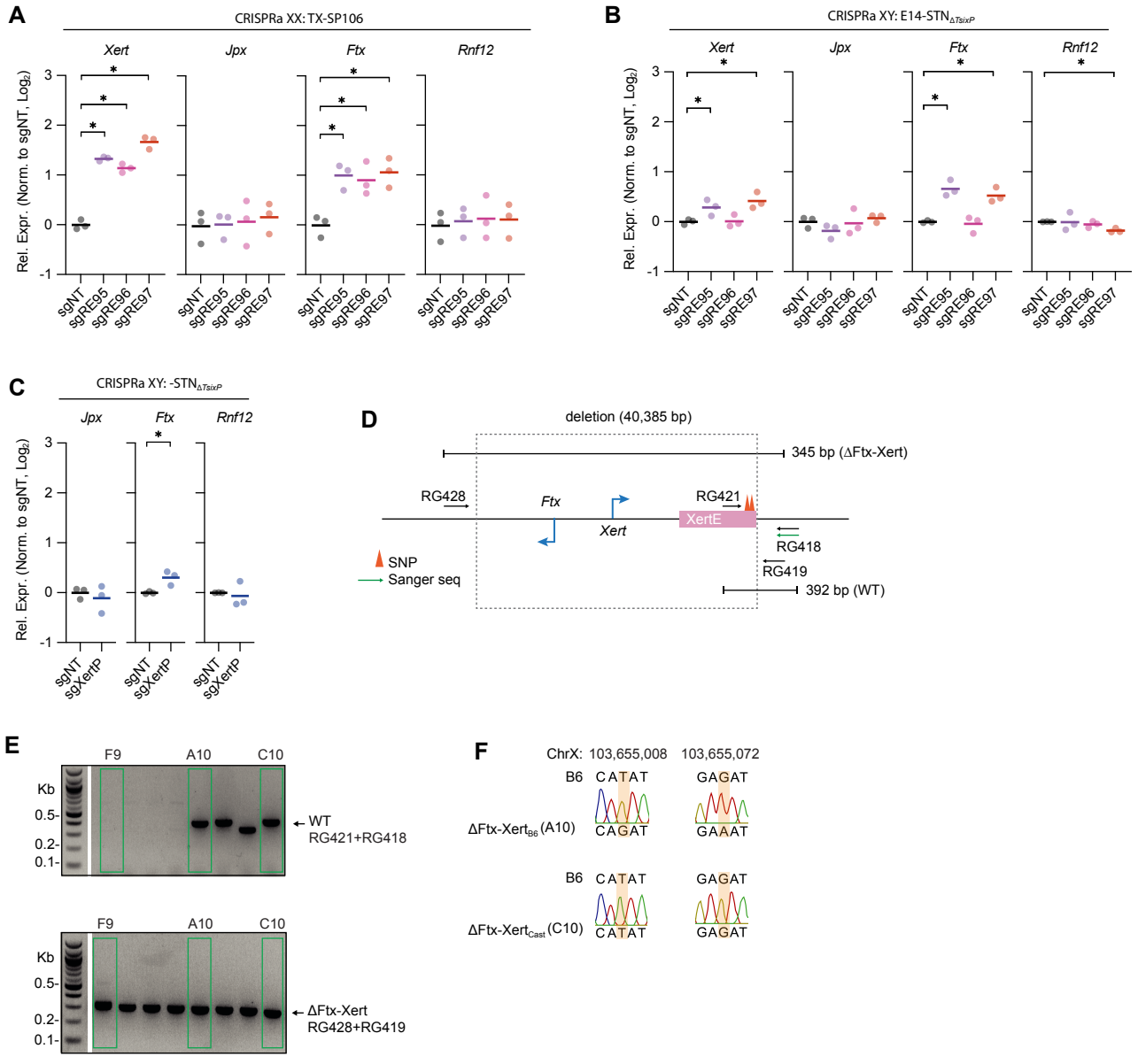
A
CRISPRa XX: TX-SP106
Xert
Jpx
Ftx
Rnf12
Rel. Expr. (Norm. to sgNT, Log2)
sgNT
sgRE95
sgRE96
sgRE97
B
CRISPRa XY: E14-STNΔTsixP
C
CRISPRa XY: -STNΔTsixP
sgXertP
D
deletion (40,385 bp)
345 bp (ΔFtx-Xert)
RG428
Ftx
Xert
RG421
XertE
RG418
RG419
392 bp (WT)
SNP
Sanger seq
E
F9
A10
C10
Kb
0.5
0.2
0.1
WT
RG421+RG418
ΔFtx-Xert
RG428+RG419
F
ChrX: 103,655,008 103,655,072
B6 CATAT GAGAT
ΔFtx-Xert B6 (A10) CAGAT GAAAT
ΔFtx-Xert Cast (C10) CATAT GAGAT

Figure S6. *Xert* and *Ftx* form a regulatory hub during initiation of XCI (Related to Figure 6).

(**A-C**) Ectopic activation of XertE (A-B) and XertP (C) through inducible CRISPR activation, using an ABA-inducible dCas9-VPR system (TX-SP106) in female (B) or a dox-inducible SunTag system in male (C) mESCs (E14-STN$_{\triangle TsixP}$). RNA expression was assessed in cells stably expressing three sgRNAs from a multiguide expression plasmid or non-targeting controls (NT) after 2 days of differentiation by qRT-PCR (n=3) and normalized to sgNT. Horizontal bars denote the mean of 3 biological replicates, dots represent individual measurements. Asterisks indicate significance of $p<0.05$ using an unpaired two-tailed *t*-test. **(D-F**) Genotyping of ΔFtx-Xert mESC lines, carrying a heterozygous or homozygous deletion of a region spanning RE84-RE97. (D) Arrows indicate primer positions. The orange pyramid indicates the SNP used to identify the wt allele by Sanger sequencing in (F). Lines indicate PCR amplicons. (E) Agarose gel images of two genotyping PCRs of ΔFtx-Xert clones with green boxes marking the clones that were selected for all further analyses. (F) Sanger sequencing of amplicon RG421/RG418 and RG418 as sequencing primer (see D) to identify the deleted allele in ΔFtx-Xert mESCs. Chromatograms of the assessed SNP (orange box) are shown with its genomic coordinate (mm10).

Figure S7

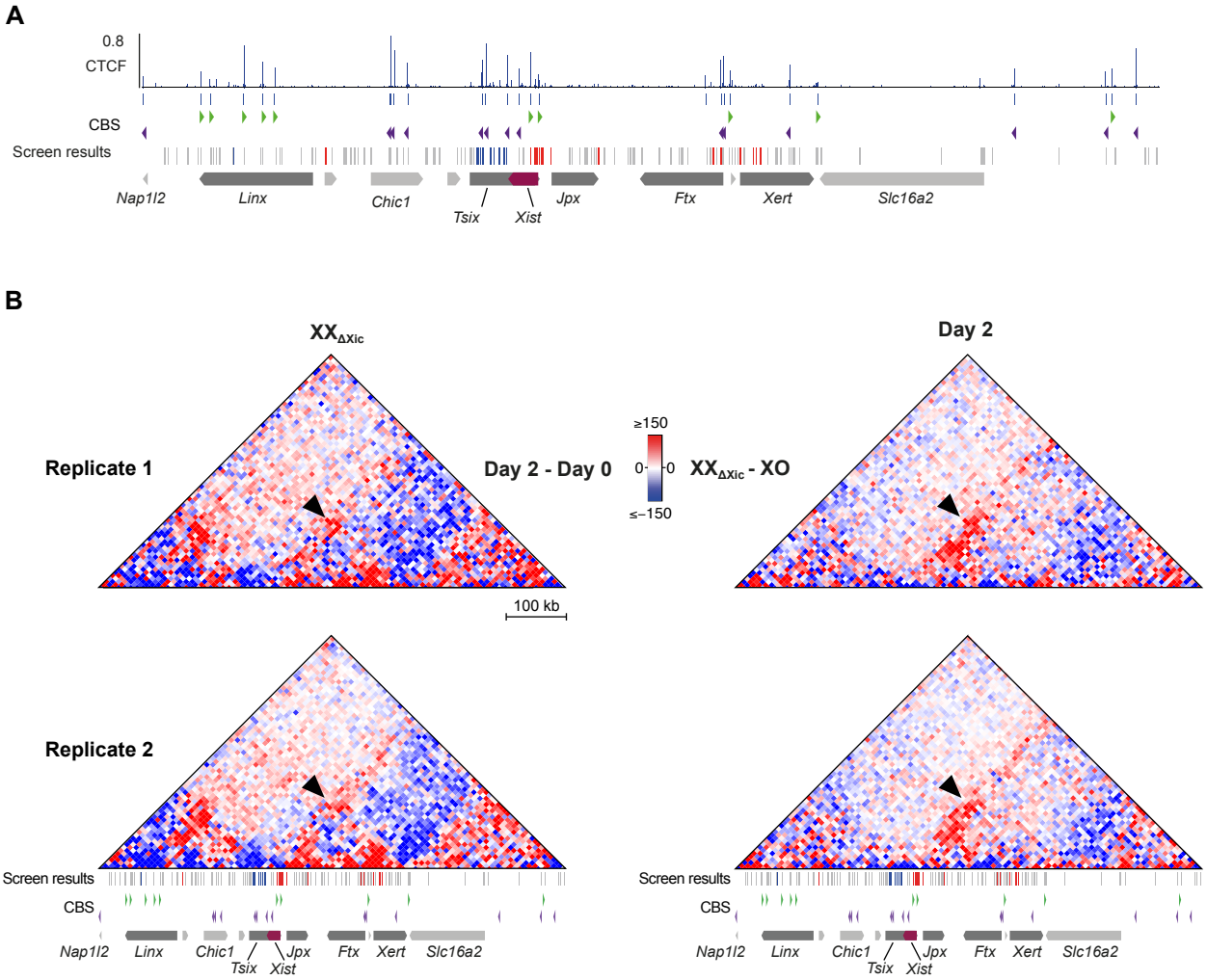
A
0.8
CTCF
CBS
Screen results
Nap1l2
Linx
Chic1
Tsix
Xist
Jpx
Ftx
Xert
Slc16a2
B
XX$_{\Delta Xic}$
Day 2
Replicate 1
Day 2 - Day 0
≥150
0
≤−150
XX$_{\Delta Xic}$ - XO
100 kb
Replicate 2
Screen results
CBS
Nap1l2
Linx
Chic1
Tsix
Xist
Jpx
Ftx
Xert
Slc16a2

Figure S7. *Xert* and *Ftx* exhibit increased contacts with the *Xist* promoter during initiation of XCI (Related to Figure 7).

(**A**) CTCF coverage track in male mESCs, derived from a published dataset (Stadler et al., 2011). Significant CTCF binding sites (CBS) are shown below the track and motif orientation is shown as triangles. The screen results are shown below the tracks, where candidate REs that inhibit (blue) or activate (red) *Xist* expression in the negative or high fractions of the CRISPR screen are colored. (**B**) Subtraction heatmaps as in Fig. 7B for two individual biological replicates comparing day 0 and 2 in $XX_{\Delta Xic}$ cells (left) and $XX_{\Delta Xic}$ and XO cells at day 2 (right).

Table S3. Comparison of CRISPR screen results with published mutant phenotypes (related to Figure 1).

While the *cis*-regulatory landscape of *Xist* has been dissected with genetic tools for more than 30 years (Galupa and Heard, 2018), we have now applied, for the first time, a high-throughput approach to allow comprehensive RE identification and quantification throughout the entire *Xic*. The CRISPRi screen we have performed relies on inactivation of promoter or enhancer elements through ectopic deposition of H3K9me3. Genomic resolution could be limited by the fact that H3K9me3 can spread over several kilobases around the targeted site (Thakore et al., 2015), which might have occurred for RE50 and RE59. Nevertheless our screen results are largely in agreement with previously reported mutant phenotypes.

ID	Annotations	Screen result	Previous finding
RE12	LinxE	repressive	repressive (Galupa et al., 2020)
RE20	Linx promoter	no effect	repressive (Galupa et al., 2020)
RE45-47	Xite (Tsix enhancer)	repressive	repressive (Ogawa and Lee, 2003)
RE49	Tsix major promoter	repressive (H3K9me3 spreading to nearby DxPas34)	no effect (Cohen et al., 2007)
RE50	adjacent to Dxpas34 (Tsix proximal enhancer)	repressive	repressive (Lee and Lu, 1999; Vigneau et al., 2006)
RE51-53	Tsix intronic elements	repressive	weakly repressive (Vigneau et al., 2006)
RE55	Xist intron 1 pluripotency factor binding site	weakly activating and repressive	weakly activating and repressive (Barakat et al., 2011; Minkovsky et al., 2013)
RE57	XistP2, CpG island, Repeat A, YY1 and CTCF binding sites	strongly activating	activating (Hoki et al., 2009; Makhlouf et al., 2014; Penny et al., 1996; Royce-Tolland et al., 2010)
RE58	Xist TSS	strongly activating	activating (Penny et al., 1996)
RE59	upstream of Xist TSS	activating (H3K9me3 spreading to nearby RE58?)	no effect (Newall et al., 2001)
RE61	Jpx promoter	activating	activating (Tian et al., 2010)
RE85-RE88	Ftx promoter (RE88 major TSS, RE85 minor TSS)	RE 85 activating; weaker effect for RE87; RE88 non-significant	activating (Furlan et al., 2018; Soma et al., 2014)
RE 127	Rnf12 promoter	activating	activating (Barakat et al., 2011; Jonkers et al., 2009)